

Magnetic field induced residual dipolar couplings of imino groups in nucleic acids from measurements at a single magnetic field

Jinfa Ying · Alexander Grishaev · Michael P. Latham · Arthur Pardi · Ad Bax

Received: 22 May 2007 / Accepted: 17 July 2007 / Published online: 7 August 2007
© Springer Science+Business Media B.V. 2007

Abstract For base-paired nucleic acids, variations in $^1J_{\text{NH}}$ and the imino ^1H chemical shift are both dominated by hydrogen bond length. In the absence of molecular alignment, the $^1J_{\text{NH}}$ coupling for the imino proton then can be approximated by $^1J_{\text{NH}} = (1.21\text{Hz/ppm})\delta_{\text{H}} - 103.5 \pm 0.6$ Hz, where δ_{H} represents the chemical shift of the imino proton in ppm. This relation permits imino residual dipolar couplings (RDCs) resulting from magnetic susceptibility anisotropy (MSA) to be extracted from measurement of ($^1J_{\text{NH}} + \text{RDC}$) splittings at a single magnetic field strength. Magnetic field-induced RDCs were measured for tRNA^{Val} and the alignment tensor determined from magnetic-field alignment of tRNA^{Val} agrees well with the tensor calculated by summation of the MSA tensors of the individual nucleobases.

Keywords Alignment · Chemical shift · Dipolar coupling · Magnetic susceptibility anisotropy · RDC · tRNA^{Val}

Electronic supplementary material The online version of this article (doi:10.1007/s10858-007-9181-7) contains supplementary material, which is available to authorized users.

Jinfa Ying, Alexander Grishaev and Michael P. Latham contributed equally to this work.

J. Ying · A. Grishaev · A. Bax (✉)
Laboratory of Chemical Physics, National Institute of Diabetes and Digestive and Kidney Diseases, National Institutes of Health, Bethesda, MD 20892, USA
e-mail: bax@nih.gov

M. P. Latham · A. Pardi (✉)
Department of Chemistry and Biochemistry, 215 UCB, University of Colorado, Boulder, CO 80309-0215, USA
e-mail: arthur.pardi@colorado.edu

For a molecule in solution, anisotropy of its molecular magnetic susceptibility leads to partial alignment in an external magnetic field, and therefore produces non-zero values for averaged second rank tensor interactions such as dipolar coupling, quadrupolar coupling, and chemical shift anisotropy (Lohman and MacLean 1978; Gayathri et al. 1982; Bothner-By et al. 1985; Kung et al. 1995; Tolman et al. 1995; Bothner-By 1996). In particular, the residual dipolar coupling (RDC) has proven to be an important parameter in characterizing both molecular structure and dynamics (Tjandra et al. 1997; Vermeulen et al. 2000; Peti et al. 2002; Prestegard et al. 2004; Blackledge 2005; Tolman and Ruan 2006). In order to achieve a higher degree of alignment, RDCs in biomolecules nowadays are most commonly measured in the presence of “alignment media”, such as liquid crystalline suspensions (Tjandra and Bax 1997; Clore et al. 1998; Hansen et al. 1998; Ruckert and Otting 2000) or anisotropically compressed acrylamide gels (Sass et al. 2000; Tycko et al. 2000). However, with the availability of increasingly stronger magnets, alignment induced by magnetic susceptibility anisotropy (MSA) gives rise to detectable RDCs even in large biomolecules despite the relatively large line widths.

Alignment resulting from magnetic susceptibility anisotropy scales with the squared value of the magnetic field strength. Although for diamagnetic systems the degree of alignment typically remains very small, even at the highest available field strengths, exploitation of MSA-alignment offers the advantage that the sample is essentially unperturbed; the interaction energy between the biomolecule and the external magnetic field is about four orders of magnitude weaker than kT. The degree of MSA-alignment tends to be considerably larger for paramagnetic molecules than for diamagnetic molecules (Tolman et al. 1995; Bertini et al. 2004), which in principle allows for the

measurement of a wide variety of homonuclear and heteronuclear RDCs for both bonded and non-bonded partners. Thus the use of paramagnetic “tagging” has recently become an attractive alternative to liquid crystalline alignment (Gaponenko et al. 2000; Ma and Opella 2000; Wohnert et al. 2003; Rodriguez-Castaneda et al. 2006). However, for diamagnetic molecules the much weaker alignment typically restricts RDC measurement to one-bond ^{15}N – ^1H and ^{13}C – ^1H interactions (Kung et al. 1995; Tjandra et al. 1996, 1997; Bryce et al. 2004; van Buuren et al. 2004).

The RDC data provide global orientational information that complements standard short-range NOE and J-coupling structural constraints. This RDC data are particularly important for solution NMR studies of nucleic acids which form extended helical structures, where there are usually very few observable NOEs between nucleotides that are separated by more than one base pair. Thus, RDC data have been used to improve the local and global structures of a wide range of nucleic acid systems ranging from DNA duplexes to a 273 nucleotide fragment of the internal ribosomal entry site RNA (Hansen et al. 1998; Lukavsky et al. 2003). Most of these studies employed external alignment media, usually Pf1 phage; however, paramagnetic and diamagnetic MSA-alignment have also been used to measure RDCs in nucleic acids (Beger et al. 1998; Al-Hashimi et al. 2001; Bryce et al. 2004). Here we present a simple method for determining imino ^{15}N – ^1H MSA-induced RDCs in nucleic acids from NMR measurements at a single magnetic field. For MSA-induced RDCs, the observed one-bond J splitting is equal to $J_{XY}(0) + D_{XY}(B_0)$ where $J_{XY}(0)$ is the J coupling between nuclei X and Y at zero magnetic field, and $D_{XY}(B_0)$ is the MSA-induced RDC between this pair of nuclei at magnetic field strength, B_0 . Since $D_{XY}(B_0)$ scales with B_0^2 , measurement of the $J_{XY}(0) + D_{XY}(B_0)$ at a minimum of two fields allows determination of both the $J_{XY}(0)$ and $D_{XY}(B_0)$ values (Gayathri et al. 1982; Bothner-By 1996). These measurements are generally performed at as different magnetic field strengths as possible to maximize the magnitude of the RDCs and also to minimize the effect of propagated measurement error on the determination of the RDCs. Here, this procedure was used to determine the imino $^1D_{\text{NH}}$ at 800 MHz for a sample of uniformly ^{15}N -enriched native *E. coli* tRNA^{Val}, and these RDCs were compared with those obtained by a new method, which calculates $^1D_{\text{NH}}$ from measurements of the $^1J_{\text{NH}}$ splitting at only a single magnetic field.

The imino ^{15}N – ^1H $^1J_{\text{NH}}$ splittings were measured by two methods and at field strengths corresponding to 500 and 800 MHz. The first method employed an ^{15}N – ^1H WATERGATE-HSQC experiment acquired without ^1H decoupling in the ^{15}N dimension (Piotto et al. 1992), which

yields a simple $^1J_{\text{NH}}$ doublet for the observed imino resonances (Fig. 1A). The second method utilized interleaved ^1H -decoupled ^{15}N – ^1H HSQC and ^{15}N – ^1H TROSY-HSQC experiments (Pervushin et al. 1998) (Fig. 1B), where the difference in peak positions in these two spectra equals $^1J_{\text{NH}}/2$. All the experiments used weak rectangular 90° and 180° ^1H pulses, with the carrier at 13 ppm and adjusted such that the first null in their excitation profiles occurs at the water resonance. In these experiments, resonances are observed for slowly exchanging imino protons involved in stable base pair or tertiary interactions (Fig. 1). The $^1J_{\text{NH}}(500)$ and $^1J_{\text{NH}}(800)$ values for the native tRNA^{Val} are given in Table 1S and represent the averaged values obtained from the two methods. Here, for brevity, $^1J_{\text{HN}}(Q)$ refers to the total $^1J_{\text{HN}}$ splitting, including the RDC, at Q MHz. The 800 MHz $^1D_{\text{NH,exp}}$ coupling is obtained from the following relation, $^1D_{\text{NH,exp}}(800) = [800^2/(800^2 - 500^2)] \times [^1J_{\text{HN}}(800) - ^1J_{\text{HN}}(500)]$. $^1J_{\text{NH,exp}}(0)$ is then calculated from $^1J_{\text{HN}}(800) - ^1D_{\text{NH,exp}}(800)$, and both the $^1J_{\text{NH,exp}}(0)$ and $^1D_{\text{NH,exp}}(800)$ data for tRNA^{Val} are reported in Table 1S.

If the $^1J_{\text{NH}}(0)$ could be independently predicted, then $^1D_{\text{NH}}(B_0)$ could be determined from data collected at a single (high) magnetic field. Dingley et al. (1999) have previously shown that there is a strong linear correlation between the one-bond imino $^1J_{\text{HN}}$ coupling and the imino proton chemical shift. Subsequent computational results

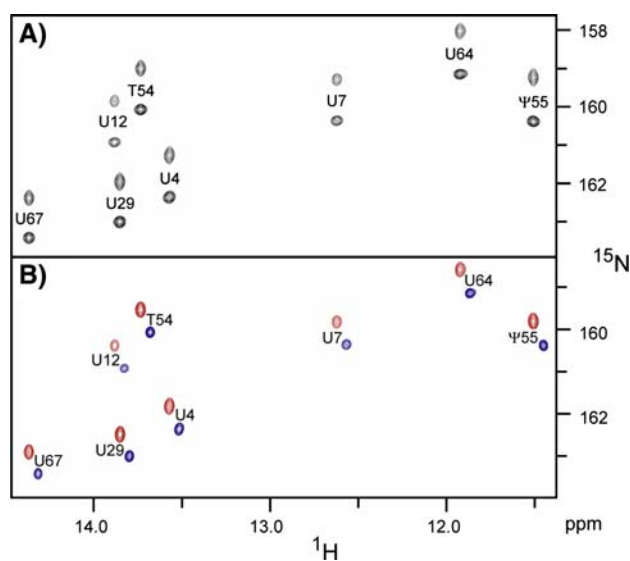


Fig. 1 Small region of the 2D ^{15}N – ^1H correlation spectra of tRNA^{Val} recorded at 800 MHz, 25°C, showing correlations for the imino groups of U nucleotides. (A) ^1H -coupled HSQC spectrum, recorded such that the ^{15}N Boltzmann component adds to the broader and weaker upfield ^{15}N – ^1H doublet component (requiring $90_x - (4^1J_{\text{NH}})^{-1} - 180_x - (4^1J_{\text{NH}})^{-1} - 90_y$ for the ^1H pulses during the initial INEPT transfer on Bruker spectrometers). (B) Superimposed ^1H -decoupled HSQC spectrum (red) and TROSY spectrum (blue)

indicated that the magnitude of the coupling is a function of the hydrogen bond length, as is the imino proton chemical shift (Dingley et al. 1999; Barfield et al. 2001). For both G and T nucleotides in a 24-nucleotide DNA triplex, the experimental $^1J_{\text{HN}}$ value was shown to follow the relation (Dingley et al. 1999; Barfield et al. 2001):

$$^1J_{\text{NH}} = (1.32 \text{ Hz/ppm})\delta_{\text{H}} - 104.79 \text{ Hz} \quad (1)$$

where δ_{H} represents the imino proton chemical shift in ppm. The $^1J_{\text{NH,calc}}(0)$ values calculated for tRNA^{Val} from Eq. 1 agree well with our experimentally determined $^1J_{\text{NH,exp}}(0)$ values in Table 1S (not shown). However, the data on the DNA triplex used to derive Eq. 1 still contain small but unknown contributions from the MSA-induced RDCs. Therefore, Eq. 1 was reparameterized using the 18 extrapolated $^1J_{\text{NH,exp}}(0)$ and δ_{H} values for tRNA^{Val}, and an additional set of 21 $^1J_{\text{NH,exp}}(0)$ and δ_{H} values collected for a 73-nt fragment of the U2-U6 spliceosomal RNA (Sashital et al. 2004). Linear fitting yields (Fig. 1S):

$$^1J_{\text{NH,calc}}(0) = (1.21 \text{ Hz/ppm})\delta_{\text{H}} - 103.5 \text{ Hz.} \quad (2)$$

Figure 2A shows there is good agreement between the $^1J_{\text{NH,calc}}(0)$ obtained from Eq. 2 and $^1J_{\text{NH,exp}}(0)$ for tRNA^{Val}. The modified nucleobases of s⁴U8 and Ψ55 gave poor fits in this correlation and were therefore excluded when parameterizing Eq. 2. Since these nucleobases have different pK_as for the imino nitrogen (Saenger 1984) leading to unusual δ_{H} values, the failure of Eq. 2 to predict their $^1J_{\text{NH}}(0)$ values is not surprising. On the other hand, for the modified nucleobase of m⁷G46, where the methyl substitution is far removed from the imino nitrogen, no unusual behavior is expected nor observed. tRNA^{Val} contains a variety of non-Watson-Crick base-base interactions (Saenger 1984) and Eq. 2 does a good job of predicting the imino $^1J_{\text{NH}}(0)$ values for these non-canonical base pairs and base triples. For example, in both the G50-U46 wobble interaction and the G15-C48 reverse Watson-Crick interaction the imino protons are hydrogen bonded to a carbonyl oxygen instead of a ring nitrogen, and these $^1J_{\text{NH}}(0)$ are well calculated by Eq. 2. The $^1J_{\text{NH}}(0)$ for T54 is also well predicted even though this base forms a reverse Hoogsteen base pair with A58, where the T imino hydrogen bonds to the N7 of A58. The imino groups for G22 and U12, which form part of the Watson-Crick interaction in two different base triples in tRNA^{Val}, also fit well to Eq. 2, consistent with previous studies of base triples by Dingley et al. (1999). The imino group of G46 forms a hydrogen bond with the N7 of G22 in the C13-G22-G46 base triple and its $^1J_{\text{NH}}(0)$ is also reasonably well predicted by Eq. 2. These results indicate that Eq. 2 represents a robust method for predicting imino $^1J_{\text{NH}}(0)$ values for bases in a wide range of base–base interactions in nucleic acids. It should be

noted that the fact that Eq. 2 was parameterized to optimize agreement between $^1J_{\text{NH,calc}}(0)$ and $^1J_{\text{NH,exp}}(0)$ has negligible impact on the correlation observed in Fig. 2A, since 39 experimental data points were used to optimize the two adjustable parameters in Eq. 2. An analogous correlation plot, where for each nucleotide $^1J_{\text{NH,calc}}(0)$ is derived from an equation parameterized by using only the 38 couplings of the remaining nucleotides, yields an essentially indistinguishable correlation (data not shown). The $^1J_{\text{NH,exp}}(0)$ and the $^1J_{\text{NH,calc}}(0)$ have a pairwise root-mean-square difference (rmsd) of 0.8 Hz. Similar measurements for the more concentrated 73-nt U2-U6 RNA yielded an even smaller rmsd of 0.6 Hz between the imino $^1J_{\text{NH,exp}}(0)$ values and those obtained from Eq. 2 (Supplementary Fig. S1).

Although the above pairwise rmsd of 0.6–0.8 Hz constitutes an upper limit for the error in the $^1J_{\text{NH,calc}}(0)$, this rmsd also includes experimental errors in the $^1J_{\text{NH,exp}}(0)$ values. Below, the latter are estimated from the reproducibility in the measured values, allowing for an estimate of the error associated with Eq. 2. For tRNA^{Val}, duplicate $^1J_{\text{HN}}$ measurements at 500 MHz yield a pairwise rmsd of 0.6 Hz, and therefore a random error of 0.3 Hz in the values averaged over the two measurements. At 800 MHz, the pairwise rmsd between the two independent measurements equals 0.8 Hz, yielding a random error of 0.4 Hz in the averaged $^1J_{\text{NH}}(800)$. Assuming that the errors at 500 and 800 MHz are uncorrelated, error propagation results in an estimated error of 0.55 Hz in the value of $^1J_{\text{HN,exp}}(0)$. With a pairwise rmsd of 0.8 Hz between this extrapolated $^1J_{\text{HN,exp}}(0)$ value and the value obtained using Eq. 2, this points to an error of 0.6 Hz between the value calculated using Eq. 2 and the true $^1J_{\text{HN}}(0)$ value. The U2-U6 RNA sample, which was about five times more concentrated than the tRNA^{Val} sample, yielded much higher signal-to-noise data and a pairwise rmsd of 0.6 Hz between $^1J_{\text{HN,exp}}(0)$ and $^1J_{\text{NH,calc}}(0)$, indicating that in this case this difference is dominated by the error associated with Eq. 2.

The purpose of obtaining $^1J_{\text{NH}}(0)$ is so that it can be used to determine $^1D_{\text{NH}}(800)$ from the measured $^1J_{\text{NH}}(800)$. Depending on whether $^1J_{\text{NH}}(0)$ is derived from the difference of the experimental $^1J_{\text{NH}}(800)$ and $^1J_{\text{NH}}(500)$ values or from Eq. 2, we refer to the corresponding $^1D_{\text{NH}}(800)$ values as $^1D_{\text{NH,exp}}(800)$ or $^1D_{\text{NH,calc}}(800)$. These values are listed in Table 1S. Figures 2B and C show singular value decomposition (SVD) fits (Losonczi et al. 1999; Sass et al. 1999) of $^1D_{\text{NH,exp}}(800)$ and $^1D_{\text{NH,calc}}(800)$ to the tRNA^{Val} structure and show comparable qualities for the fits. This holds true for both a homology model of tRNA^{Val} (coordinates available as Supplementary Material), based on the X-ray structure of tRNA^{Phe} (Table 1), and a tRNA^{Val} model that was generated by rigid body refinement using RDCs measured in

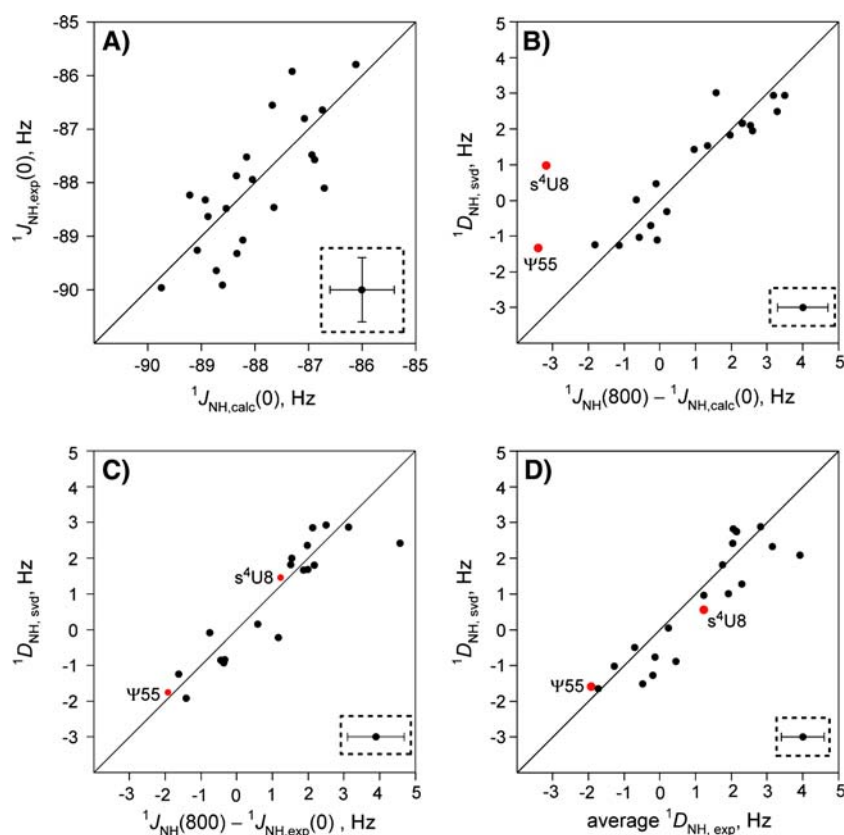


Fig. 2 Scatter plots of imino ^{15}N - ^1H couplings in tRNA^{Val} . (A) Plot of $^1J_{\text{NH}}(0)$ values obtained from extrapolation to zero field of the $^1J_{\text{NH}}$ splittings measured at 800 and 500 MHz ^1H frequency versus values derived using Eq. 2. (B) Plot of the field-induced RDCs at 800 MHz, obtained from $^1J_{\text{NH}}$ splittings measured at 800 MHz and use of Eq. 2, versus values obtained by SVD fitting to a homology model of tRNA^{Val} , based on the X-ray structure of tRNA^{Phe} . The two outliers (colored in red) were excluded from the SVD. (C) Plot of the field-induced RDCs at 800 MHz, where $^1J_{\text{NH}}(0)$ is obtained from

extrapolation of $^1J_{\text{NH}}$ splittings measured at 800 and 500 MHz, versus values obtained by SVD fitting. Note that the experimental RDCs for $\text{s}^4\text{U8}$ and $\Psi55$ fit well with the structure and were included in the SVD, even though they have a negligible effect on the SVD-derived alignment parameters. (D) Plot of RDCs, averaged over the two sets of values shown in (B) and (C), versus values obtained by SVD fitting to the homology model of tRNA^{Val} . For $\text{s}^4\text{U8}$ and $\Psi55$, $^1J_{\text{NH}}(0)$ values obtained from extrapolation of $^1J_{\text{NH}}$ splittings measured at 800 and 500 MHz were used instead

liquid crystalline alignment media (Vermeulen et al. 2005) (Supplementary Table 2S). After averaging of the corresponding $^1D_{\text{NH,exp}}(800)$ and $^1D_{\text{NH,calc}}(800)$ values, a small improvement in the SVD fit is observed (Fig. 2D, Table 1), resulting from the fact that the errors in $^1D_{\text{NH,exp}}(800)$ and $^1D_{\text{NH,calc}}(800)$ are partially uncorrelated.

The field-induced alignment tensor of tRNA^{Val} can also be predicted by summing the group susceptibility

anisotropies of the individual nucleic acid bases, using axially symmetric susceptibility tensors previously parameterized for DNA (Bryce et al. 2004). Both the magnitude and orientation of the predicted alignment tensor are in good agreement with the one obtained by SVD fitting, as reflected in very similar values for the alignment strength D_{a}^{NH} and rhombicity, and a high value (0.987) of the normalized scalar product (Sass et al. 1999) between

Table 1 Comparison of alignment tensors for tRNA^{Val} induced by molecular magnetic susceptibility anisotropy, and by liquid crystalline Pf1^a

Method	Base MSA-prediction	SVD fit to $^1D_{\text{NH,calc}}$	SVD fit to $^1D_{\text{NH,exp}}$	SVD fit to $^1D_{\text{NH,ave}}$	SVD fit to Pf1-induced RDCs
D_{a}^{NH} , Hz	1.31 ^b	1.51	1.47	1.50	15.33
Rhombicity	0.29	0.13	0.48	0.33	0.66
Q factor		0.45	0.49	0.40	0.28

^a The liquid crystalline solution contained approximately 20 mg/mL Pf1. The MSA-alignment tensor corresponds to the alignment at 800 MHz ^1H frequency, i.e., to $^1J_{\text{HN}}(800) - ^1J_{\text{HN}}(0)$

^b A 1.041 Å N–H bond length was used for calculating the predicted D_{a}^{NH} value

the predicted and best-fitted alignment tensor (Table 1). Interestingly, even though tRNA^{Val} is rather large (76 nucleotides), the magnitude of the MSA-induced alignment tensor is relatively small, comparable to what is seen for the B-form DNA Dickerson dodecamer (Bryce et al. 2004). The reason for this modest alignment is the near orthogonal orientation of the two main stems of the L-shaped tRNA, which causes partial cancellation of the MSA-induced alignments. With the magnetic susceptibility of the nucleobases being negative, this L-shape results in an alignment tensor that has its largest principal axis orthogonal to the plane of the L, which contrasts with the alignment observed for tRNA in Pf1 medium.

Our results demonstrate that even the relatively small MSA-induced RDCs contain valuable structural information for larger RNAs, and that Eq. 2 represents a valid method for determining imino $^1D_{NH}$ in nucleic acids. Even if the imino $^1D_{NH}$ values were determined from measurements at multiple magnetic fields, Fig. 2D shows that when averaging $^1D_{NH,calc}$ and $^1D_{NH,exp}$, an even better SVD fit to the structure is obtained. Furthermore, Eq. 2 appears to be valid for a variety of hydrogen bonded imino interactions including G-U wobble pairs, various base triples and non-canonical base pairs.

The results presented here show that measurement of $^1J_{NH}$ at two or more magnetic fields is no longer a prerequisite for obtaining MSA-induced RDCs for the imino groups of nucleic acids. The use of Eq. 2 to independently determine $^1J_{NH}(0)$ facilitates the determination of $^1D_{NH}(B_0)$ without any discernable increase in error compared to determining $^1J_{NH}(0)$ from measurements at two magnetic fields. Moreover, the data here indicate that $^1J_{NH}(0)$ can be calculated from Eq. 2 for a variety of base pair and tertiary interactions.

Acknowledgement This work was supported in part by the Intramural Research Program of the NIDDK, NIH, and by the Intramural AIDS-Targeted Antiviral Program of the Office of the Director, NIH, and NIH grant AI33098 (AP); MPL was supported in part by a NIH Training Grant T32 GM65103. We thank Dr. Sam E. Butcher and Dipa Sashital for providing us with the ^{15}N -enriched U2-U6 sample.

References

- Al-Hashimi HM, Tolman JR, Majumdar A, Gorin A, Patel DJ (2001) Determining stoichiometry in homomultimeric nucleic acid complexes using magnetic field induced residual dipolar couplings. *J Am Chem Soc* 123:5806–5807
- Barfield M, Dingley AJ, Feigon J, Grzesiek S (2001) A DFT study of the interresidue dependencies of scalar J-coupling and magnetic shielding in the hydrogen-bonding regions of a DNA triplex. *J Am Chem Soc* 123:4014–4022
- Beger RD, Marathias VM, Volkman BF, Bolton PH (1998) Determination of internuclear angles of DNA using paramagnetic assisted magnetic alignment. *J Magn Reson* 135:256–259

- Bertini I, Del Bianco C, Gelis I, Katsaros N, Luchinat C, Parigi G, Peana M, Provenzani A, Zoroddu MA (2004) Experimentally exploring the conformational space sampled by domain reorientation in calmodulin. *Proc Natl Acad Sci USA* 101:6841–6846
- Blackledge M (2005) Recent progress in the study of biomolecular structure and dynamics in solution from residual dipolar couplings. *Prog Nucl Magn Reson Spectrosc* 46:23–61
- Bothner-By AA (1996) Magnetic field induced alignment of molecules. In: Grant DM, Harris RK (eds) *Encyclopedia of nuclear magnetic resonance*, vol 5. Wiley, Chichester, pp 2932–2938
- Bothner-By AA, Gayathri C, Van Zijl PCM, Maclean C, Lai JJ, Smith KM (1985) High-field orientation effects in the high-resolution proton NMR-spectra of diverse porphyrins. *Magn Reson Chem* 23:935–938
- Bryce DL, Boisbouvier J, Bax A (2004) Experimental and theoretical determination of nucleic acid magnetic susceptibility: importance for the study of dynamics by field-induced residual dipolar couplings. *J Am Chem Soc* 126:10820–10821
- Clore GM, Starich MR, Gronenborn AM (1998) Measurement of residual dipolar couplings of macromolecules aligned in the nematic phase of a colloidal suspension of rod-shaped viruses. *J Am Chem Soc* 120:10571–10572
- Dingley AJ, Masse JE, Peterson RD, Barfield M, Feigon J, Grzesiek S (1999) Internucleotide scalar couplings across hydrogen bonds in Watson-Crick and Hoogsteen base pairs of a DNA triplex. *J Am Chem Soc* 121:6019–6027
- Gaponenko V, Dvoretzky A, Walsby C, Hoffman BM, Rosevear PR (2000) Calculation of z-coordinates and orientational restraints using a metal binding tag. *Biochemistry* 39:15217–15224
- Gayathri C, Bothner-By AA, Van Zijl PCM, Maclean C (1982) Dipolar magnetic-field effects in NMR-spectra of liquids. *Chem Phys Lett* 87:192–196
- Hansen MR, Mueller L, Pardi A (1998) Tunable alignment of macromolecules by filamentous phage yields dipolar coupling interactions. *Nat Struct Biol* 5:1065–1074
- Kung HC, Wang KY, Goljer I, Bolton PH (1995) Magnetic alignment of duplex and quadruplex DNAs. *J Magn Reson Ser B* 109:323–325
- Lohman JAB, MacLean C (1978) Alignment effects on high resolution NMR spectra induced by the magnetic field. *Chem Phys* 35:269–274
- Losonczi JA, Andrec M, Fischer MWF, Prestegard JH (1999) Order matrix analysis of residual dipolar couplings using singular value decomposition. *J Magn Reson* 138:334–342
- Lukavsky PJ, Kim I, Otto GA, Puglisi JD (2003) Structure of HCVIRES domain II determined by NMR. *Nat Struct Biol* 10:1033–1038
- Ma C, Opella SJ (2000) Lanthanide ions bind specifically to an added “EF-hand” and orient a membrane protein in micelles for solution NMR spectroscopy. *J Magn Reson* 146:381–384
- Pervushin KV, Wider G, Wuthrich K (1998) Single transition-to-single transition polarization transfer (ST2-PT) in [N-15,H-1]-TROSY. *J Biomol NMR* 12:345–348
- Peti W, Meiler J, Bruschweiler R, Griesinger C (2002) Model-free analysis of protein backbone motion from residual dipolar couplings. *J Am Chem Soc* 124:5822–5833
- Piotto M, Saudek V, Sklenar V (1992) Gradient-tailored excitation for single-quantum NMR spectroscopy of aqueous solutions. *J Biomol NMR* 2:661–665
- Prestegard JH, Bougault CM, Kishore AI (2004) Residual dipolar couplings in structure determination of biomolecules. *Chem Rev* 104:3519–3540
- Rodriguez-Castaneda F, Haberz P, Leonov A, Griesinger C (2006) Paramagnetic tagging of diamagnetic proteins for solution NMR. *Magn Reson Chem* 44:S10–S16

- Ruckert M, Otting G (2000) Alignment of biological macromolecules in novel nonionic liquid crystalline media for NMR experiments. *J Am Chem Soc* 122:7793–7797
- Saenger W (1984). Principles of nucleic acid structure. Springer Verlag, New York
- Sashital DG, Cornilescu G, Butcher SE (2004) U2-U6 RNA folding reveals a group II intron-like domain and a four-helix junction. *Nat Struct Mol Biol* 11:1237–1242
- Sass H-J, Musco G, Stahl SJ, Wingfield PT, Grzesiek S (2000) Solution NMR of proteins within polyacrylamide gels: diffusional properties and residual alignment by mechanical stress or embedding of oriented purple membranes. *J Biomol NMR* 18:303–309
- Sass J, Cordier F, Hoffmann A, Rogowski M, Cousin A, Omichinski JG, Lowen H, Grzesiek S (1999) Purple membrane induced alignment of biological macromolecules in the magnetic field. *J Am Chem Soc* 121:2047–2055
- Tjandra N, Bax A (1997) Direct measurement of distances and angles in biomolecules by NMR in a dilute liquid crystalline medium. *Science* 278:1111–1114
- Tjandra N, Grzesiek S, Bax A (1996) Magnetic field dependence of nitrogen-proton J splittings in N-15-enriched human ubiquitin resulting from relaxation interference and residual dipolar coupling. *J Am Chem Soc* 118:6264–6272
- Tjandra N, Omichinski JG, Gronenborn AM, Clore GM, Bax A (1997) Use of dipolar ^1H - ^{15}N and ^1H - ^{13}C couplings in the structure determination of magnetically oriented macromolecules in solution. *Nat Struct Biol* 4:732–738
- Tolman JR, Flanagan JM, Kennedy MA, Prestegard JH (1995) Nuclear magnetic dipole interactions in field-oriented proteins: information for structure determination in solution. *Proc Natl Acad Sci USA* 92:9279–9283
- Tolman JR, Ruan K (2006) NMR residual dipolar couplings as probes of biomolecular dynamics. *Chem Rev* 106:1720–1736
- Tycko R, Blanco FJ, Ishii Y (2000) Alignment of biopolymers in strained gels: a new way to create detectable dipole-dipole couplings in high-resolution biomolecular NMR. *J Am Chem Soc* 122:9340–9341
- van Buuren BNM, Schleucher J, Wittmann V, Griesinger C, Schwalbe H, Wijmenga SS (2004) NMR spectroscopic determination of the solution structure of a branched nucleic acid from residual dipolar couplings by using isotopically labeled nucleotides. *Angew Chem Int Ed* 43:187–192
- Vermeulen A, McCallum SA, Pardi A (2005) Comparison of the global structure and dynamics of native and unmodified tRNA. *Biochemistry* 44:6024–6033
- Vermeulen A, Zhou H, Pardi A (2000) Determining DNA global structure and DNA bending by application of NMR residual dipolar couplings. *J Am Chem Soc* 122:9638–9647
- Wohnert J, Franz KJ, Nitz M, Imperiali B, Schwalbe H (2003) Protein alignment by a coexpressed lanthanide-binding tag for the measurement of residual dipolar couplings. *J Am Chem Soc* 125:13338–13339